

N=Z Waiting Point Nucleus ^{68}Se : Collective Rotation and High-K Isomeric States

Yang Sun¹, Zhanwen Ma¹, Ani Aprahamian², Michael Wiescher²

¹*Department of Physics and Astronomy, University of Tennessee, Knoxville, Tennessee 37996*

²*Department of Physics, University of Notre Dame, Notre Dame, Indiana 46556*

(November 21, 2018)

The structure of collective states and quasi-particle excitations in ^{68}Se is analyzed by using the projected shell model. It is found that the $g_{9/2}$ orbitals play a decisive role for the structure of this nucleus. At the prolate minimum, alignment of the low-K states causes the observed first backbending in moment of inertia and we predict a second backbending that has not yet been reported. At the oblate minimum, quasi-particles having high-K can form long-lived isomeric states. The structure of ^{68}Se is discussed with respect to the isomers and their possible impact on the determination of its nuclear mass.

PACS: 21.60.Cs, 23.20.Lv, 26.30.+k, 27.50.+e

Thermonuclear runaways on the surface of neutron stars have been identified as energy sources for type I X-ray bursts [1–3]. The explosive conditions resulting from the thermonuclear runaway provide the site for rapid sequences of successive proton captures (rp-process) resulting in the creation of nuclei far beyond ^{56}Ni all the way to the proton rich regions [4] of the chart of nuclides.

X-ray bursts are observed frequently [5], yet the nucleosynthesis and the correlated energy generation is not completely understood. In addition to the uncertainty of the astrophysical conditions, network simulations of the rp-process are hindered by the lack of experimental information on the structure of nuclei along the rp-process path [4,6]. Nuclei of particular interest to the rp-process are the N=Z waiting point nuclei [6]. These are the nuclei where further p-capture typically leads to a p-unbound isotone or where the Q value for the (p, γ) reaction is low making the reverse reaction possible. In order for the rp-process to continue, it needs to wait for β -decay or for the 2p-capture to bridge the waiting point. The time spent at these N=Z waiting points is strongly dependent on the photodisintegration rates, the β -decay lifetimes, and particularly on the masses of nuclei along the path.

The mass of ^{68}Se is particularly relevant to determining whether further p-capture is likely to occur. There have been several attempts [7] to measure the half-life of ^{69}Br by fragmentation studies at GANIL and MSU. No ^{69}Br was observed but an upper limit of 150ns was set for the half-life. The implication is that ^{69}Br should be p-unbound. This implies that the rp-process should proceed via 2p-capture or β -decay of ^{68}Se . There are some new mass measurements [8] of several N=Z nuclei in the A=80 mass region from GANIL. The measurement involves the use of the CSS2 cyclotron at GANIL as a high resolution mass spectrometer. The relative mass differences of unknown and known nuclei are determined from their differences in times of flight in the CSS2. The mass excess measured for ^{68}Se was -52.347 ± 0.080 MeV. If one now uses the measured ^{68}Se mass, the implication is that ^{69}Br should be bound by greater than 1 MeV. This result is of course inconsistent with the fragmentation experi-

ments. One possible explanation for the discrepancy in the measurements would be if the GANIL mass measurement was that of an isomeric state in ^{68}Se .

The purpose of this Letter is to investigate the role of the structure of ^{68}Se for the mass measurements and therefore for the rp-process. We analyze the structure of both collective and quasi-particle excitations in ^{68}Se using the projected shell model (PSM) [9] with the idea of looking for the feasibility of the existence of isomeric states in this nucleus.

Great progress has been made on the theory side by the application of advanced shell model diagonalization methods which can explicitly yield the structure wave functions, and matrix elements for even-even, odd-A, and odd-odd nuclei. One successful example is the application of the spherical pf-shell model developed by the Strasbourg-Madrid group [10]. By employing this model, Langanke and Martínez-Pinedo have demonstrated its strength in understanding the nuclear processes that govern those violent astrophysical phenomena [11].

The rp-process path involves nuclei which are significantly deformed. At the deformed potential minimum, abnormal high- j orbitals such as $g_{9/2}$ intrude into the pf-shell near the Fermi level. Therefore, the $g_{9/2}$ orbitals have to be included in the model space for the present interest. This strongly suggests proper selection of a shell model basis that is capable of describing the undergoing physics within a manageable space.

The PSM [9] is a shell model diagonalization method which adopts the bases from the well-established Nilsson model with pairing correlation incorporated into them by a BCS calculation. The selection of the bases is first implemented in the multi-quasiparticle (qp) basis with respect to the deformed BCS vacuum $|0\rangle$; then the broken rotational symmetry is recovered by angular momentum projection technique [9] to form a shell model basis in the laboratory frame. Finally a shell model Hamiltonian is diagonalized in the projected space. The problem of dimensionality that is often tied with conventional shell-model calculations does not occur in the PSM.

In the present PSM calculation for ^{68}Se , particles in

three major shells ($N = 2, 3, 4$) for both neutron and proton are activated. The shell model space includes the 0-, 2- and 4-qp states:

$$\left\{ |0\rangle, \alpha_{n_i}^\dagger \alpha_{n_j}^\dagger |0\rangle, \alpha_{p_i}^\dagger \alpha_{p_j}^\dagger |0\rangle, \alpha_{n_i}^\dagger \alpha_{n_j}^\dagger \alpha_{p_i}^\dagger \alpha_{p_j}^\dagger |0\rangle \right\}, \quad (1)$$

where α^\dagger is the creation operator for a qp and the index n (p) denotes neutron (proton) Nilsson quantum numbers which run over properly selected (low-lying) orbitals. Note that the index i and j in Eq. (1) are general. For example, a 2-qp state can be of positive parity if both quasiparticles i and j are from the same major shell; it can also be of negative parity if two quasiparticles are from two neighboring major shells. Positive and negative parity states span the whole configuration space with the corresponding matrix in a block-diagonal form classified by the parity.

As the first step in a PSM calculation, one has to find out where the optimal basis is. The shape coexistence feature in ^{68}Se seems to be firmly suggested by the recent experimental data of Fischer *et al.* [12]. Two coexisting rotational bands were identified, with the ground state band having properties consistent with collective oblate rotation, and the excited band having characteristics consistent with prolate rotation. Constrained Hartree-Fock calculations by Sarriguren *et al.* [13] also found coexistence of two energy minima in ^{68}Se , with the oblate solution as the ground state, in supporting the experimental conclusion. Moreover, the observed bands are found to interact rather weakly indicating a high energy barrier [12]. The theoretical barrier between the two well-separated minima is calculated as about 3 MeV [13]. These evidences suggest a possible simplification in our calculation that we can perform the diagonalization separately at the prolate and oblate minimum by neglecting the coupling between the two minima. Collecting all of the above information, we thus perform the following PSM calculations at $\varepsilon_2 = 0.28$ for the prolate states, and $\varepsilon_2 = -0.24$ for the oblate states.

It is evident from the experimental data [12] that the rotational states in ^{68}Se are dominated by quadrupole collectivity and pairing interactions. To describe these properties, it is efficient to use a quadrupole plus pairing Hamiltonian [9]

$$\hat{H} = \hat{H}_0 - \frac{1}{2}\chi \sum_{\mu} \hat{Q}_{\mu}^\dagger \hat{Q}_{\mu} - G_M \hat{P}^\dagger \hat{P} - G_Q \sum_{\mu} \hat{P}_{\mu}^\dagger \hat{P}_{\mu}, \quad (2)$$

where \hat{H}_0 is the spherical single-particle Hamiltonian which contains a proper spin-orbit force, whose strengths (i.e. the Nilsson parameters) are taken from Ref. [14]. The second term in the Hamiltonian is the quadrupole-quadrupole interaction and the last two terms are the monopole and quadrupole pairing interactions, respectively. The interaction strength χ is determined by the self-consistent relation such that the

input quadrupole deformation ε_2 and the one resulting from the HFB procedure coincide with each other [9]. The monopole pairing strength G_M is taken to be $G_M = [18.0 - 14.5(N - Z)/A]/A$ for neutrons and $G_M = 14.5/A$ for protons. Finally, the quadrupole pairing strength G_Q is assumed to be proportional to G_M , the proportionality constant being fixed to 0.20 in the present work. These interaction strengths are consistent with the values used in the previous PSM calculations for this mass region [15,16].

The eigenvalue equation of the PSM for a given spin I takes the form [9]

$$\sum_{\kappa'} \{ H_{\kappa\kappa'}^I - E^I N_{\kappa\kappa'}^I \} F_{\kappa'}^I = 0. \quad (3)$$

The expectation value of the Hamiltonian with respect to a ‘‘rotational band κ ’’ $H_{\kappa\kappa}^I/N_{\kappa\kappa}^I$ defines a band energy, and when plotted as functions of spin I , we call it a band diagram [9]. A band diagram displays bands of various configurations before they are mixed by the diagonalization procedure of Eq. (3). Irregularity in a spectrum may appear if a band is crossed by another one(s) at a certain spin.

Fig. 1(a) shows our results for the lowest states of each spin, and at the prolate and oblate minima. They are presented in the plots of moment of inertia vs. square of rotational frequency. Remarkable agreement has been obtained for the oblate band. Our calculations suggest a gradual increase in the moment of inertia extended to higher spin states beyond the current experimental band. The basic features of the moment of inertia in the observed prolate band has also been reproduced. In addition to the sharp backbending at $I = 8$ that has been observed, we predict a second sharp backbending at $I = 16$. We note that the highest spin state in the measurement of this band was $I = 14$. Extension of the current experiment to higher spins can thus test our prediction.

In Fig. 1(b), calculated $B(E2)$ values are plotted for the prolate and oblate bands. These values have not been measured experimentally. We found that in the oblate band, the $B(E2)$ values gradually increase until they are saturated at $I = 14$. In the prolate band, however, drastic variations are predicted. Sudden drops in the curve appear at spins $I = 8$ and $I = 16$, corresponding to the two places where the moment of inertia bends back. From both the moment of inertia and $B(E2)$ values, it is thus interesting to see that the co-existing bands in one nucleus exhibit very distinct characteristics where the prolate band is highly irregular and the oblate one is rather smooth.

These interesting observations can be understood by studying the band diagrams. We found that the $g_{9/2}$ orbitals play a decisive role for the near yrast structure of this nucleus. Close to the neutron and proton Fermi levels of ^{68}Se , single qp states of $g_{9/2}$ with different K

quantum numbers are split by the deformed potential. At the prolate minimum, the Fermi levels are surrounded by the low-K states, whereas at the oblate minimum, they are near the high-K states. The low- and high-K states respond rather differently to the rotation, which is reflected in very different pair alignment processes.

In Fig. 2, various configurations are distinguished by different types of lines. The symbols represent the yrast states obtained after the configuration mixing. There are more than 20 bands in each calculation, but only representative ones are displayed for discussion. Note that for the 2-qp bands, there are two closely-lying bands (a neutron and a proton band) because they nearly coincide with each other for the entire spin region.

Fig. 2(a) shows the band diagram calculated at the oblate minimum. There are two 2-qp bands starting at about 5 MeV. These two 2-qp bands (one neutron and one proton band) are based on the $g_{9/2}$ quasiparticles with $K = 7/2$ and $9/2$, coupled to $K = 1$. As spin increases, they gradually approach the g-band, and finally cross with it between $I = 14$ and 16 . The band crossing is so gentle with a very small crossing angle that one cannot see a band disturbance in the yrast solution. In fact, rather smooth behavior has been predicted for the yrast band in both moment of inertia and $B(E2)$ values (see Fig. 1). On the other hand, the two $g_{9/2}$ quasiparticles with $K = 7/2$ and $9/2$ can also couple to a 2-qp state with a total $K = 8$. The $K = 8$ bands have similar band-head energies as the $K = 1$ bands since they originate in the same two $g_{9/2}$ quasiparticles.

Fig. 2(b) presents the band diagram at the prolate minimum. In this case, the two $g_{9/2}$ quasiparticles with low-K quantum numbers $K = 1/2$ and $3/2$ lie close to the Fermi energy, and 2-qp bands involving these low-K states behave very differently from the oblate case. It can be seen that the two 2-qp bands (again, one neutron- and one proton-band) based on the low-K $g_{9/2}$ quasiparticles (coupled to $K = 1$) sharply cross the g-band at $I = 8$. Because of this crossing, the g-band is disturbed, resulting in the observed first bandbending (see Fig. 1(a)). The crossing changes also the g-band dominance in the yrast wave functions before the crossing to the 2-qp band dominance after the crossing, which leads to the sudden drop in the $B(E2)$ values (see Fig. 1(b)).

A 4-qp state can be formed by coupling of the neutron and the proton 2-qp states discussed above. As shown by the dashed-dotted curve in Fig. 2(b), the 4-qp band can sharply cross the 2-qp bands between $I = 14$ and 16 , and dominates the yrast wave functions thereafter. The crossing will result in the second backbending in moment of inertia, as shown in Fig. 1(a), and a bigger drop in $B(E2)$ values at $I = 16$, as predicted in Fig. 1(b). The highest spin state of the current experimental data for this band is $I = 14$ [12]. Extension of a few high spin states will be a crucial test of our predictions, thus the correctness of the band crossing interpretation for ^{68}Se .

The theoretical energy spectrum at the oblate minimum is shown in Fig. 3 in comparison with available data [12]. We predict two nearly-degenerate (only one of them is shown here) high-K bands ($K = 8$) with a bandhead spin $I = 8$ and an excitation energy of 5 MeV. They are long-lived isomeric states in the sense that no allowed γ -transition matrix elements of low multipolarity can connect these states to the nearby g-band ($K = 0$). Our calculation shows the high-K band at a lower excitation energy than any other 2-qp bands. Step-wise transitions via other multi-qp states are also unlikely since there are no other nearby states available. Thus, once the isomeric $I = 8$ states are populated, the high-K states find no path for further γ -decay.

Our prediction on the high-K isomeric states was based on a realistic calculation that has reasonably reproduced all the known structure data in this nucleus. However, we should mention two possible caveats. First, these isomers are based on 2-qp states of the $g_{9/2}$ orbitals. Therefore, correct single-particle energies of the neutron and proton $g_{9/2}$ orbitals are important. In the present calculation, we employed the newly-adjusted Nilsson parameters [14] which were obtained by a best estimation for the proton $g_{9/2}$ energy. Thus, further experimental data regarding an accurate proton $g_{9/2}$ position are very much desired. Second, neutron-proton pairing has not been explicitly considered in our theory. An interesting aspect in our case is that if the proton-neutron pairing interaction is included in our Eq. (2), the two nearly-degenerate 2-qp states will no longer be proton or neutron 2-qp state, but a superposition of them. The interaction will generally push one of them down, and the other up, thus modifying their positions. Experimentally, if one would observe only one of them, that could be a signature of the proton-neutron pairing effect which may not be sensitively felt by the ground state.

The occurrence of the $I = 8$ isomers that lie very close to the yrast band may have a significant impact on the mass measurement for this nucleus, and a significant influence on the resulting abundances of the rp-process. The possibility that the GANIL measurement [8] has hit any isomeric state with an excitation greater than 1 MeV would explain the discrepancy with the fragmentation experiments. It should be noted also that the shape isomer, the lowest state in the prolate minimum, which has not been seen in Ref. [12], lies possibly at about 1 MeV excitation [13]. Thus, experimentally searching for these isomeric states is very important.

In summary, we calculate the structure of ^{68}Se using the PSM. Our results show excellent agreement with recent experimental findings regarding the spectroscopy of this nucleus: the coexisting oblate and prolate minima, the backbend at $I = 8$. We further predict an additional backbend at $I = 16$ and a number of high K isomers at approximately 5 MeV above the ground state. The existence of isomeric states in this nucleus may provide

resolution for the observed differences between the different types of measurements, and it may play a significant role in the mass flow and therefore resulting abundances of the rp-process. The latter point will be investigated further via network calculations of the rp-process.

Valuable discussions with J.A. Sheikh and C.J. Lister are acknowledged. Y.S. thanks the colleagues at the University of Notre Dame for their warm hospitality, where this collaboration was initiated. The support of the National Science Foundation under grant PHY 99-01133 and the graduate school of the University of Notre Dame are gratefully acknowledged.

-
- [1] S.E. Woosley and R.E. Taam, *Nature* **263**, 101 (1976).
 - [2] L. Maraschi and A. Cavaliere, *Highlights of Astronomy* **4**, 127 (1977).
 - [3] P. Joss, *Nature* **280**, 310 (1977).
 - [4] L. Van Wormer *et al.*, *Astrophys. J.* **432**, 326 (1994).
 - [5] L. Bildsten and T. Strohmayer, *Physics Today*, **40**, February (1999).
 - [6] H. Schatz, *et al.*, *Phys. Rep.* **294**, 167 (1998).
 - [7] B. Blank *et al.*, *Phys. Rev. Lett.* **66**, 1571 (1991); **74**, 4611 (1995); D.J.Morrissey *et al.*, *Proceedings of the International Conference on Exotic Nuclei and Atomic Masses*, 303 (1995).
 - [8] A.S. Lalleman, Ph.D. dissertation, GANIL (2000).
 - [9] K. Hara and Y. Sun, *Int. J. Mod. Phys.* **E4**, 637 (1995).
 - [10] E. Caurier *et al.*, *Phys. Rev.* **C50**, 225 (1994).
 - [11] K. Langanke and G. Martínez-Pinedo, *Nucl. Phys.* **A673**, 481 (2000).
 - [12] S.M. Fischer *et al.*, *Phys. Rev. Lett.* **84**, 4064 (2000).
 - [13] P. Sarriguren, E. Moya de Guerra and A. Escuderos, *Nucl. Phys.* **A658**, 13 (1999).
 - [14] Y. Sun *et al.*, *Phys. Rev.* **C62**, 021601(R) (2000).
 - [15] J. Döring *et al.*, *Phys. Rev.* **C57**, 2912 (1998).
 - [16] R. Palit *et al.*, *Nucl. Phys.* **A686**, 141 (2001).

FIG. 1. (a) Moments of inertia $\frac{2I-1}{E(I)-E(I-2)}$ as function of ω^2 with $\omega = \frac{E(I)-E(I-2)}{2}$ (The experimental data are taken from Ref. [12]), and (b) calculated B(E2) values.

FIG. 2. Band diagrams (bands before configuration mixing) and the lowest band after configuration mixing (denoted by symbols) for ^{68}Se at (a) the oblate minimum, and (b) the prolate minimum. Only the important lowest-lying bands in each configuration are shown.

FIG. 3. Calculated energy spectrum for ^{68}Se at the oblate minimum. High-K isomeric states are predicted. Results are compared with data (denoted by stars) whenever levels are experimentally known [12].

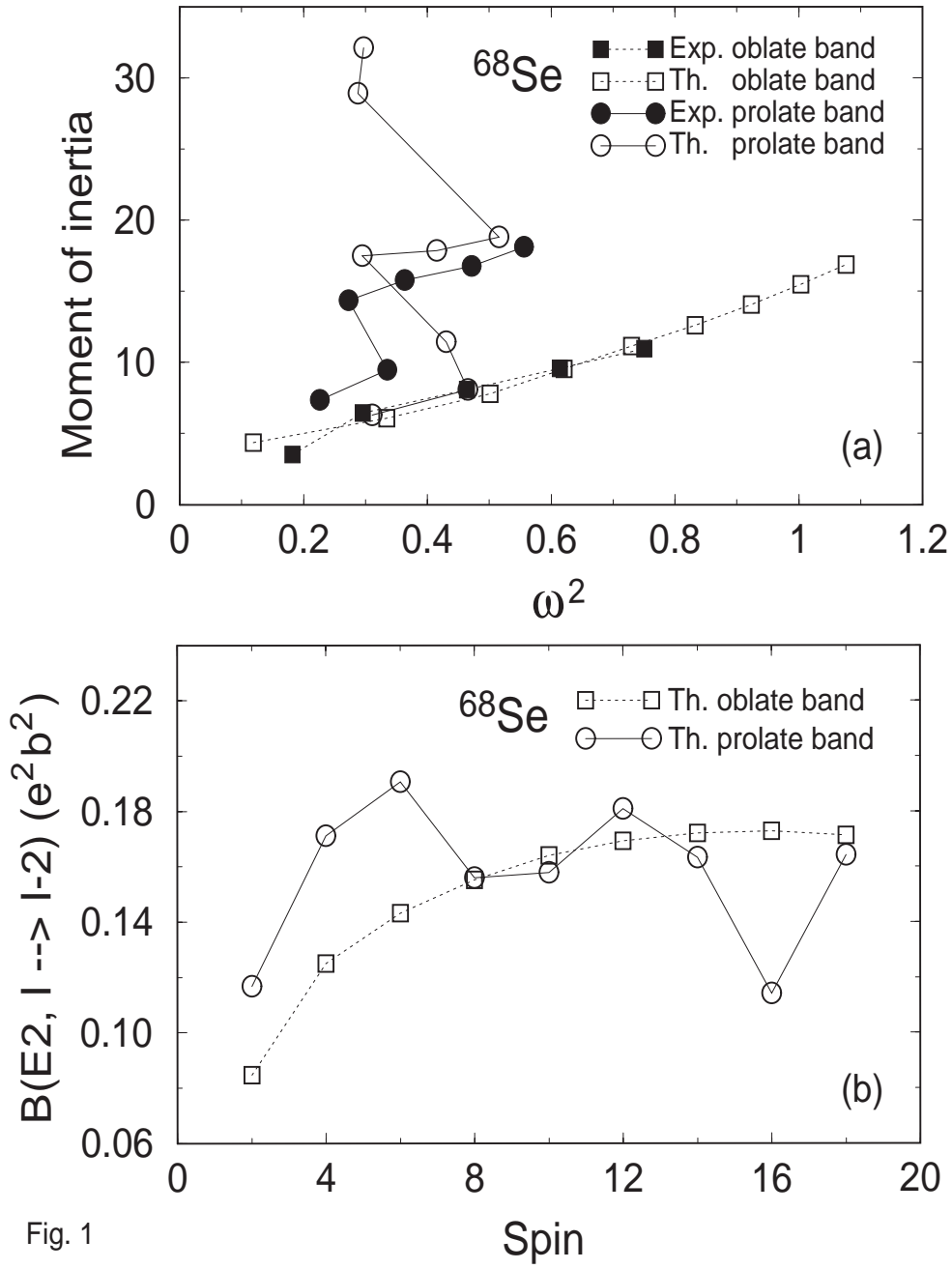
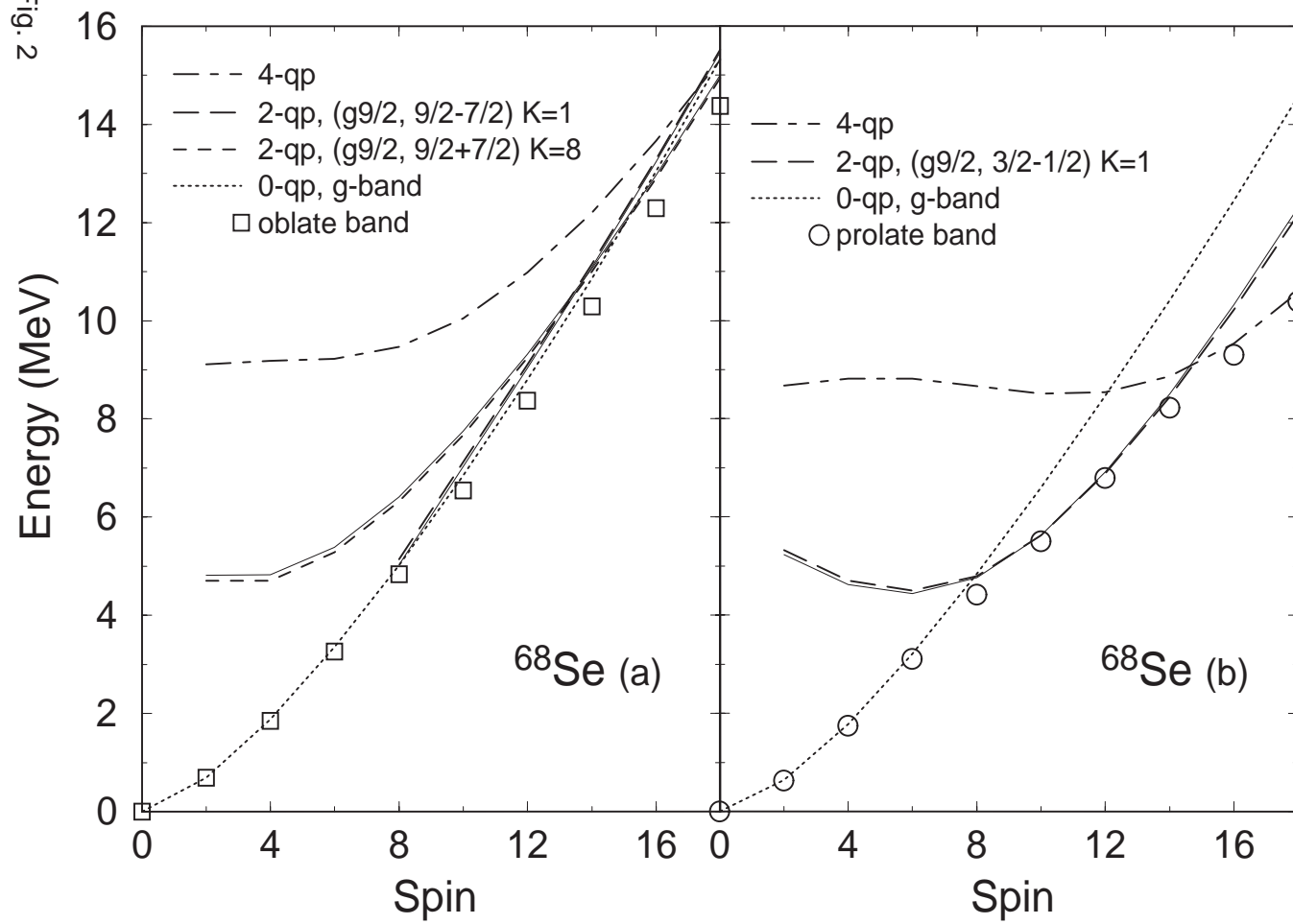


Fig. 1

Fig. 2



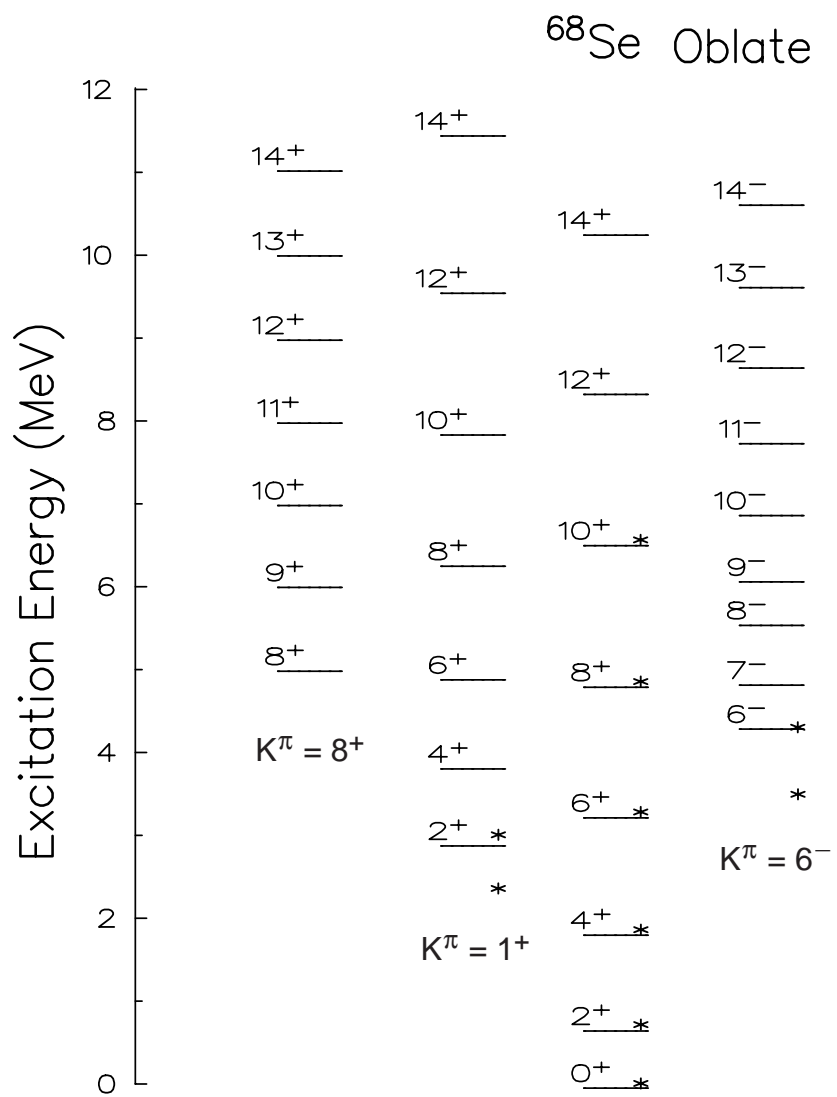


Fig. 3